Monatshefte für Chemie 105, 689—711 (1974)

Thermodynamic Properties of Cobalt—Selenium Alloys*

By

H. Jelinek and **K. L. Komarek**

Institute of Inorganic Chemistry, University of Vienna, Vienna, Austria

With 6 Figures

(Received March 25, 1974)

Vapor pressures of selenium in cobalt—selenium alloys were determined by an isopiestic method between 600 and 1000 °C and between 52 and 66.6 at% Se. Activities of selenium were evaluated according to three methods taking into account the complexity of the selenium vapor. For the nonstoichiometric $Co_{1-x}Se$ phase with NiAs-type structure a statistical model was applied. Activities and partial molar enthalpies of selenium derived by assuming random distribution of cobalt atoms and cobalt vacancies in the 001/2-layers of the NiAs-lattice are in very good agreement with the experimental values. The interaction energy between cobalt vacancies was found to be 7780 cal/g-atom.

In a continuation of the thermodynamic investigations of transition metal—chalcogen alloys[1, 2] the study was extended to the cobalt—selenium system. The partial Co—Se phase diagram described in various compilations[3–5] and mostly based on thermoanalytical investigations of *Hashimoto*[6], and of *Dudkin* and *Vaidanich*[7], is characterized by the nonstoichiometric compound $Co_{1-x}Se$ of hexagonal B 8-C 6-type structure[8, 9] and by cubic pyrite-type $CoSe_2$[10–12]. The results were largely confirmed by X-ray diffraction studies of *Bøhm* et al.[13], who observed an additional, third compound, Co_9Se_8, with fcc pentlandite-type structure. At 600 °C they found for $Co_{1-x}Se$ a continuous transformation from the hexagonal (from 50.5 to 53.5 at % Se) to the monoclinic (from 53.5 to 57.8 at % Se) symmetry.

At lower temperature the homogeneous $Co_{1-x}Se$ phase region splits into a hexagonal γ-phase and a monoclinic γ'-phase with a miscibility gap which closes at 530 °C[14, 15]. Instead of nonstoichiometric $Co_{1-x}Se$ *Igaki* and *Noda*[16, 17] reported the existence of three

* Dedicated to Prof. *E. Hayek* on the occasion of his 70th birthday.

distinct phases, $CoSe_{1.03}$, $CoSe_{1.13}$, and $CoSe_{1.30}$, with a maximum melting point of 1055 °C at 53.0 at % Se.

Komarek and Wessely[18] constructed the complete Co—Se phase diagram, based on *DTA*- and X-ray measurements. Above 1448 °C there is a miscibility gap in cobalt-rich melts, above 952 °C another one in melts with more than 70 at % Se. $Co_{1-x}Se$ has a congruent melting point at 54.0 at % Se and 1078 °C and a maximum range of homogeneity between 50.7 at % Se at 910 °C and 59 at % Se at 952 °C. α-Co and $Co_{1-x}Se$ form a eutectic at 44.5 at % Se and 910 °C. Co_9Se_8 decomposes by a peritectoid reaction at 420 °C[19] into α-Co and $Co_{1-x}Se$, and $CoSe_2$ decomposes peritectically at 938 °C into $Co_{1-x}Se$ and a Se-rich melt. *Cambi* et al.[20] studied the thermal decomposition of $CoSe_2$ but their results do not agree with the established phase diagram.

Thermodynamic information on Co—Se alloys has been until recently virtually non existent. The enthalpy of formation of "CoSe" was determined by *Fabre*[21] using solution calorimetry at 25 °C as -18.0 kcal mol^{-1} and *Karapet'yants*[22] estimated the standard free energy of formation of CoSe at 25 °C to be -9.7 kcal mol^{-1}. *Eror* and *Wagner*[23] determined the vapor pressure of some alloys between 50.0 and 71.2 at % Se by the dew point method but they did not succeed in obtaining vapor pressure data for alloys with a selenium content less than 62.3 at% Se. Recently *Laffitte* and *Cerclier*[14, 15] determined activities of Co from 50.5 to 67.3 at% Se between 400 and 600 °C using a solid electrolyte *emf* method. *Matlasevich* et al.[24, 25] measured Co activities between 51.7 and 66.7 at% Se and 360° and 550 °C by an *emf* method with a liquid electrolyte. *Feenberg* and *Vaisburd*[26] employed an *emf* method to obtain activities of Co in Co—Se melts at 1300 °C between 35 and 50 at% Se. *Mills*[27] has critically evaluated the thermodynamic data of Co—Se alloys based on data published in literature[13, 14, 16, 21, 23].

In the present investigation thermodynamic activities of selenium of solid Co—Se alloys were determined by an isopiestic method. Cobalt specimens were equilibrated in a temperature gradient with selenium vapor from a source kept at the temperature minimum.

Experimental Procedure

The materials were 99.999 percent selenium shots (American Smelting and Refining Corp., New York) and 0.1 mm thick 99.9 percent cobalt foil (Sherritt Gordon Mines Ltd., Canada) with the following impurities (in per cent): 0.1 Ni, 0.014 C, 0.018 Fe, 0.004 S, 0.005 Cu.

The cobalt foil was punched into anular rings (20 mm OD, 11 mm ID) which were then cleaned in CCl_4 and acetone. They were weighed on a semi-microbalance to an accuracy of ± 0.05 mg, put into graphite crucibles, and then reweighed. All graphite parts were machined from high-purity

high-density (1.92 g cm^{-3}) graphite rods (United Carbon Products Corp., U.S.A.) and were heated before use at 1000 °C in vacuum (10^{-3} torr) for three hours. The graphite crucibles (25 mm OD, 1.5 mm wall thickness) had press-fit lids and a hole (7 mm D) in the center for the quartz thermocouple well. All quartz parts were cleaned in hot cleaning solution, rinsed with distilled water, and dried. They were then evacuated to 10^{-3} torr, heated for three hours at 1000 °C, and back-filled with argon at 800 °C. The quartz crucible (35 mm OD, 100 mm high) with selenium ($\approx$ 30 g) was at the bottom of the quartz equilibration tube (42 mm OD, 2 mm wall thickness, $\approx$ 500 mm long) which was connected at the top by a ground quartz joint to a vacuum system. 20 to 25 graphite crucibles separated by graphite spacers were stacked on the quartz thermocouple well (5 mm OD) which reached into a slightly larger quartz well placed into the center of the selenium reservoir. The quartz thermocouple well was fused at the top to a larger quartz tube (35 mm OD). The position of the graphite crucibles with respect to the selenium reservoir was measured to within $\pm$ 0.5 mm. The equilibration tube was repeatedly evacuated and filled with argon and finally sealed to the quartz tube attached to the top of the thermocouple well under a vacuum of 10^{-4} torr.

The equilibration tube was inserted in a vertical resistance furnace with two separately controlled windings. The end with the selenium reservoir was surrounded by a Cu cylinder (80 mm high) to give a zone of constant temperature ($\pm$ 0.5 °C). The temperature of the two windings was controlled by Ni/Cr-Ni thermocouples connected to single-point controllers (Type Bitric M 1, Hartmann & Braun, Frankfurt, BRD). The temperature of the samples and of the reservoir was determined by moving a Pt/Pt-10 percent Rh thermocouple up and down the quartz thermocouple well with a motor and by synchronously registering the output of the thermocouple with a recording arrangement previously described[28]. The thermocouple was calibrated against the freezing points of high-purity Cd, Zn, Sb, Ag, and Cu by the standard NBS procedure[29]. An experiment lasted for several weeks and was terminated by quenching the tube in water and by simultaneously inserting a Cu-rod into the quartz thermocouple well. The samples were weighed and put back into the furnace for one more week under identical conditions. If the samples showed no further weight change, the length of the treatment was taken as having been sufficient for equilibration. The selenium content of the samples was calculated from the weight difference. In separate tests it was ascertained that heating Co foil in a graphite crucible at 1000 °C for three weeks and a graphite crucible in selenium vapor at 900 °C for two weeks did not produce any noticeable weight changes of the Co foil and of the graphite crucible, resp. The composition of the samples was also checked by chemical analysis. The specimens were dissolved in aqua regia and excess HNO_3 was destroyed by evaporation. Hexamethylene tetramine was added as a buffer to the dilute aqueous solution and Co determined by titration with a 10^{-2}M-*EDTA* solution using methylthymol blue as an indicator. Co contents by chemical analyses agreed with those by weight changes within $\pm$ 0.3 percent.

X-ray powder patterns were taken in a 57 mm Debye-Scherrer camera using CoK_α radiation with a Fe-filter. The reflexes of the hexagonal NiAs-phase were evaluated by extrapolating the curves of lattice parameter vs $\frac{1}{2}$ ($\cos^2\delta/\sin\delta + \cos^2\delta/\delta$) towards $\delta = 90°$.

Table 1. *Experimental Isopiestic Results in the* Co—Se *System*

Number	Temp., (°C)	at% Se	$-\log a_{Se} - \Delta\bar{H}_{Se}$ (Method A)		$-\log a_{Se} - \Delta\bar{H}_{Se}$ (Method B)		$-\log a_{Se} - \Delta\bar{H}_{Se}$ (Method C)	
			Run 1					
1	938	51.87	2.183	21.36	2.035	18.89	2.223	19.05
2	934	51.91	2.177	21.36	2.028	18.88	2.213	19.04
3	927	52.02	2.164	21.36	2.014	18.86	2.203	19.02
4	920	52.06	2.152	21.35	2.000	18.85	2.191	19.01
5	909	52.18	2.131	21.35	1.977	18.84	2.169	18.99
6	902	52.32	2.120	21.34	1.964	18.82	2.156	18.97
7	888	52.55	2.094	21.32	1.934	18.79	2.129	18.93
8	878	52.63	2.075	21.31	1.913	18.77	2.109	18.91
9	860	52.87	2.040	21.30	1.873	18.74	2.072	18.87
10	847	53.00	2.013	21.30	1.842	18.72	2.041	18.84
11	824	53.34	1.967	21.26	1.789	18.67	1.990	18.75
12	807	53.54	1.931	21.24	1.747	18.63	1.947	18.71
13	777	54.07	1.864	21.17	1.669	18.48	1.866	18.57
14	750	54.55	1.801	21.09	1.594	18.28	1.783	18.45
15	709	55.45	1.698	20.90	1.472	17.83	1.652	18.15
16	681	56.32	1.623	20.58	1.381	17.38	1.553	17.82
Res.	318	—						
			Run 2					
1	972	52.13	1.957	21.35	1.820	18.84	2.012	19.00
2	963	52.23	1.943	21.35	1.805	18.82	2.001	18.98
3	950	52.40	1.922	21.34	1.781	18.81	1.988	18.95
4	946	52.42	1.914	21.34	1.773	18.80	1.970	18.94
5	935	52.54	1.894	21.32	1.751	18.79	1.948	18.93
6	921	52.78	1.871	21.31	1.724	18.76	1.924	18.88
7	907	52.96	1.846	21.30	1.696	18.72	1.897	18.85
8	897	53.10	1.828	21.28	1.675	18.70	1.879	18.81
9	881	53.29	1.797	21.26	1.640	18.67	1.849	18.77
10	870	53.40	1.777	21.25	1.617	18.65	1.826	18.75
11	850	53.70	1.737	21.22	1.572	18.60	1.783	18.67
12	838	53.88	1.713	21.20	1.544	18.55	1.756	18.63
13	815	54.28	1.664	21.14	1.488	18.40	1.699	18.52
14	798	54.53	1.628	21.09	1.446	18.28	1.657	18.44
15	768	55.17	1.561	20.96	1.367	17.97	1.572	18.25
16	747	55.68	1.511	20.82	1.308	17.72	1.507	18.06
17	708	56.70	1.351	20.40	1.191	17.20	1.381	17.65
18	685	57.50	1.242	19.80	1.117	16.80	1.301	17.15
Res.	360	—						
			Run 3					
1	964	52.57	1.736	21.31	1.601	18.79	1.803	18.93
2	952	52.84	1.716	21.31	1.579	18.75	1.781	18.87
3	947	52.89	1.707	21.31	1.570	18.74	1.774	18.85
4	938	53.10	1.692	21.29	1.552	18.70	1.758	18.81
5	931	53.17	1.680	21.28	1.539	18.69	1.745	18.79

Table 1 (continued)

Number	Temp., (°C)	at% Se	$-\log a_{Se}$ (Method A)	$-\Delta\bar{H}_{Se}$ (Method A)	$-\log a_{Se}$ (Method B)	$-\Delta\bar{H}_{Se}$ (Method B)	$-\log a_{Se}$ (Method C)	$-\Delta\bar{H}_{Se}$ (Method C)
6	918	53.43	1.657	21.25	1.513	18.65	1.722	18.74
7	909	53.50	1.641	21.25	1.495	18.64	1.705	18.70
8	893	53.80	1.612	21.21	1.462	18.57	1.674	18.62
9	880	54.00	1.588	21.17	1.435	18.52	1.649	18.60
10	860	54.20	1.549	21.15	1.390	18.43	1.608	18.51
11	845	54.40	1.519	21.12	1.356	18.35	1.588	18.46
12	812	54.95	1.450	21.02	1.276	18.08	1.496	18.32
13	788	55.42	1.398	20.90	1.215	17.84	1.425	18.17
14	747	56.40	1.302	20.55	1.122	17.35	1.302	18.78
15	725	57.11	1.248	20.13	1.038	17.41	1.241	17.41
Res.	395	—						
				Run 4				
1	950	53.77	1.339	21.21	1.208	18.58	1.411	18.66
2	946	53.88	1.332	21.20	1.200	18.55	1.406	18.62
3	939	53.95	1.320	21.19	1.187	18.53	1.392	18.61
4	932	54.10	1.308	21.16	1.173	18.47	1.381	18.57
5	924	54.24	1.294	21.15	1.158	18.42	1.365	18.53
6	915	54.39	1.278	21.12	1.140	18.36	1.351	18.49
7	905	54.59	1.260	21.09	1.118	18.27	1.331	18.43
8	897	54.63	1.246	21.08	1.103	18.25	1.316	18.42
9	885	54.86	1.223	21.04	1.078	18.14	1.292	18.35
10	877	54.92	1.207	21.02	1.059	18.11	1.276	18.33
11	861	55.30	1.177	20.94	1.025	17.90	1.243	18.20
12	849	55.50	1.153	20.88	0.998	17.80	1.218	18.13
13	841	55.62	1.137	20.85	0.979	17.74	1.199	18.08
14	818	56.02	1.090	20.71	0.924	17.53	1.145	17.92
15	788	56.87	1.024	20.28	0.848	17.22	1.066	17.57
16	772	57.40	0.987	19.90	0.805	16.85	1.019	17.22
17	750	58.32	0.936	18.75	0.745	16.40	0.954	16.32
Res.	469	—						
				Run 5				
1	964	53.25	1.514	21.27	1.383	18.68	1.568	18.82
2	955	53.32	1.499	21.26	1.367	18.67	1.569	18.76
3	951	53.40	1.491	21.25	1.358	18.66	1.563	18.75
4	944	53.51	1.481	21.24	1.346	18.64	1.551	18.72
5	938	53.60	1.470	21.23	1.335	18.62	1.540	18.70
6	928	53.70	1.452	21.22	1.314	18.59	1.522	18.68
7	920	53.90	1.438	21.20	1.298	18.54	1.508	18.62
8	903	54.15	1.408	21.16	1.264	18.46	1.475	18.55
9	892	54.30	1.388	21.14	1.242	18.40	1.434	18.52
10	872	54.60	1.350	21.08	1.199	18.26	1.416	18.43
11	858	54.90	1.322	21.02	1.167	18.22	1.385	18.34
12	831	55.30	1.268	20.94	1.105	17.90	1.325	18.20
13	811	55.63	1.226	20.84	1.056	17.73	1.276	18.08
14	780	56.28	1.158	20.61	0.977	17.42	1.194	17.82

Table 1 (continued)

Number	Temp., (°C)	at% Se	$-\log a_{Se}$ (Method A)	$-\Delta\bar{H}_{Se}$	$-\log a_{Se}$ (Method B)	$-\Delta\bar{H}_{Se}$	$-\log a_{Se}$ (Method C)	$-\Delta\bar{H}_{Se}$
15	761	56.90	1.114	20.27	0.925	17.10	1.136	17.55
16	728	64.51	0.997		0.787		0.986	
17	688	66.67	0.929		0.706		0.898	
18	654	66.70	0.833		0.593		0.769	
19	632	66.75	0.766		0.517		0.679	
20	598	66.80	0.658		0.398		0.538	
21	575	66.90	0.577		0.319		0.438	
Res.	437	—						
				Run 6				
1	1003	53.60	1.175	21.24	1.058	18.61	1.240	18.70
2	1000	53.78	1.171	21.21	1.053	18.59	1.234	18.65
3	995	53.85	1.163	21.20	1.045	18.56	1.226	18.63
4	989	54.01	1.153	21.17	1.034	18.51	1.217	18.59
5	982	54.13	1.142	21.16	1.022	18.46	1.206	18.56
6	975	54.25	1.131	21.15	1.010	18.41	1.193	18.53
7	966	54.42	1.116	21.11	0.993	18.34	1.180	18.48
8	959	54.50	1.105	21.10	0.980	18.30	1.167	18.45
9	948	54.62	1.087	21.08	0.961	18.25	1.147	18.42
10	940	54.74	1.073	21.05	0.943	18.19	1.133	18.38
11	927	54.95	1.049	21.01	0.919	18.08	1.010	18.32
12	917	55.18	1.033	20.96	0.900	17.96	1.193	18.25
13	901	55.35	1.003	20.92	0.867	17.87	1.064	18.18
14	889	55.43	0.982	20.90	0.842	17.84	1.039	18.15
15	867	55.93	0.939	20.75	0.794	17.58	0.995	17.97
16	852	56.34	0.910	20.58	0.761	17.38	0.964	17.82
17	821	57.21	0.846	20.05	0.688	16.98	0.891	17.35
18	801	57.87	0.804	19.37	0.639	16.60	0.842	16.80
19	769	66.20	0.732		0.557		0.752	
20	753	66.66	0.694		0.514		0.704	
21	722	66.73	0.617		0.429		0.607	
22	708	66.78	0.581		0.389		0.559	
23	681	66.80	0.509		0.315		0.469	
24	666	66.83	0.466		0.275		0.416	
25	638	66.86	0.384		0.205		0.308	
26	623	66.97	0.336		0.170		0.254	
Res.	527	—						

Experimental Results

A total of six experiments lasting from four to eight weeks were carried out. Reservoir temperatures ranged between 318 and 527 °C, sample temperatures between 570 and 1000 °C, and temperature gradients between 480 and 620 °C.

The experimental data for all specimens are listed in Table 1. Sample compositions, and sample and reservoir temperatures, superimposed

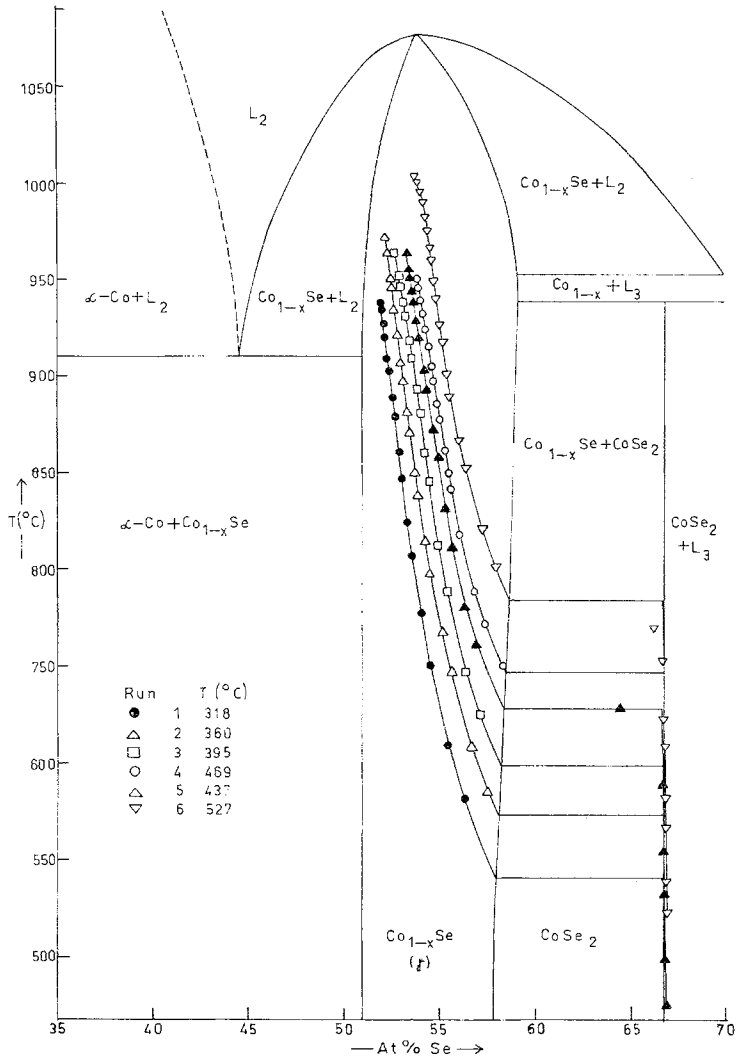

Fig. 1. Specimen composition versus specimen temperature and partial Co—Se phase diagram

on the partial phase diagram[18], are shown in Fig. 1. Run one and two were quenched after two weeks, the samples weighed, and treated again one week under the same experimental conditions. Samples in

the $Co_{1-x}Se$ phase field showed no change in weight and had attained equilibrium but those in the $CoSe_2$ range increased in weight and were

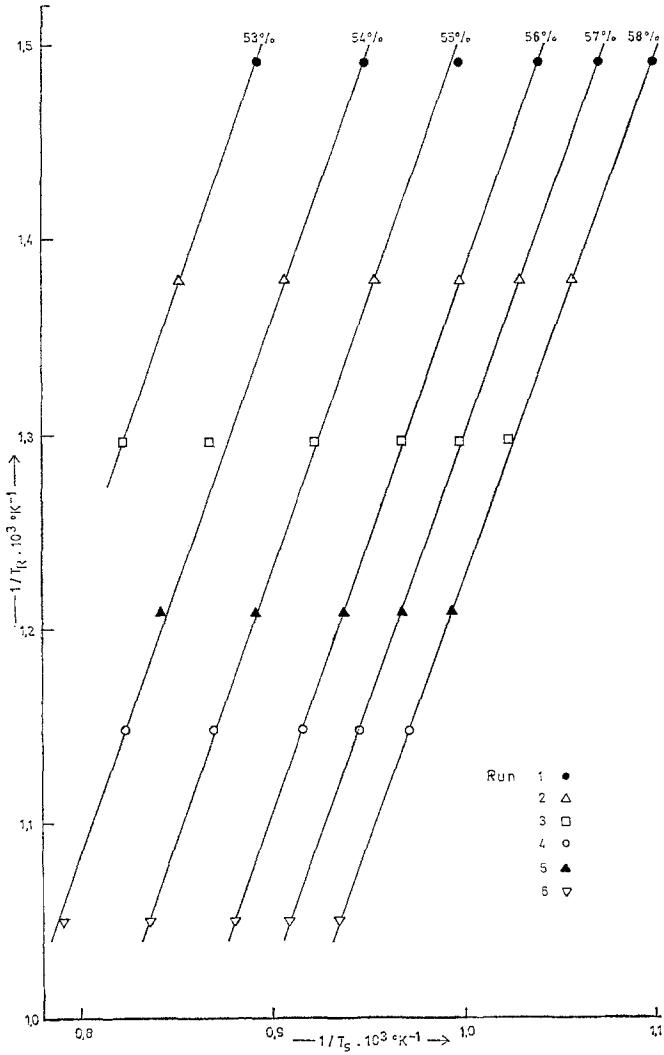

Fig. 2. Reciprocal reservoir temperature versus reciprocal sample temperature

therefore not equilibrated. Heat treatment for another week showed similar effects. These samples were used in run three and four with higher reservoir temperatures but after two weeks it was still not possible to bring the $CoSe_2$ phase into equilibrium. Non-equilibration

of the specimens in the $CoSe_2$ range, however, did not affect equilibration of samples in the $Co_{1-x}Se$ field. Run five and six were quenched after seven weeks. A further treatment of one more week did not produce weight changes of any samples, indicative of complete equilibration. According to X-ray powder patterns sample 16 of run five and sample 19 of run six were two-phase ($Co_{1-x}Se$ and $CoSe_2$). These specimens must be practically at the phase boundary so that slight temperature fluctuations will cause their compositions to change back and forth within the two-phase region.

The selenium-rich phase boundary of the $Co_{1-x}Se$ phase is in excellent agreement with the results of *Bøhm* et al.[13] of 57.8 at% Se at 600 °C and of *Komarek* and *Wessely*[18] of 59.0 at% Se at 952 °C. The cobalt-rich boundary of the $Co_{1-x}Se$ phase could not be determined since it was not possible to attain the necessary temperature gradients with the present equipment. The equilibrium curves of run five and six indicate a small range of homogeneity for $CoSe_2$ which extends from 66.7 to 67.0 at% Se and is clearly situated at the selenium-rich side of the stoichiometric composition. In Fig. 2 reciprocal reservoir temperatures (T_R) are plotted versus reciprocal specimen temperatures (T_S). Data points for alloys of equal composition lie on straight lines which proves that the results are consistent.

The evaluation of the activities in the isopiestic method is based on the fact that the vapor pressure in the equilibration tube is determined by the volatile pure component at the reservoir temperature. In equilibrium the vapor pressure of the volatile component of each alloy sample will therefore be equal to the vapor pressure of the pure component at the temperature minimum, T_R.

The activity of the volatile component of an equilibrated sample, a_i, is given by

$$a_i = \left(\frac{p\,(i_n)\,(\text{at}\,T_S)}{p^\circ\,(i_n)\,(\text{at}\,T_S)} \right)^{1/n} \tag{1}$$

If there is only one molecular species, i_n, in the vapor phase, then

$$p(i_n)\,(\text{at}\,T_S) = p^\circ(i_n)\,(\text{at}\,T_R) \tag{2}$$

and activities can be directly calculated from the saturation vapor of the volatile component.

Furthermore, partial molar enthalpies $\Delta \overline{H_i}$ can be obtained from plots like Fig. 2 using a form of the Clausius-Clapeyron equation

$$\frac{1}{T_R} = \frac{(\Delta H^\circ_{\text{ev}} - n\,\Delta \overline{H}_i)}{\Delta H^\circ_{\text{ev}} \cdot T_S} + C \tag{3}$$

with $\Delta H^\bullet_{\text{ev}}$ the enthalpy of evaporation of the pure volatile component.

Selenium vapor, however, contains all species between Se_2 and Se_8[30], the vapor composition will therefore change with temperature, and the calculation of the Se activities from isopiestic experiments employing temperature gradients will be much more complicated. Since no direct measurements of the composition of Se vapor as a function of temperature have been made in the temperature range of our experiments, three different methods of calculation were employed.

In method A it was assumed that only Se_2 is present in the vapor phase which as a first approximation seems justified at least at high temperatures since the vapor composition is shifting with increasing temperature more and more towards Se_2[30, 31]. Activities were calculated from Eqs. (1) and (2) with $n = 2$ using for the total pressure of Se *Baker's* results[32]

$$\log p^\circ (\Sigma\, Se_n) = -5043/T + 5.265 \text{ (atm)} \tag{4}$$

which are good agreement with the data of *Brebrick*[33] and *Brooks*[34].

Method B is based on empirical equations derived by *Rau*[31] from measurements of the average molecular weight of the Se vapor and of the total vapor pressure of Se. The empirical equations were obtained by curve-fitting as if only Se_2, Se_4, Se_6, and Se_8 were present in the vapor. The total vapor pressure is then given by

$$p = p(Se_2) + p(Se_2)^2/A + p(Se_2)^3/B + p(Se_2)^4/C \tag{5}$$

with

$$\log A = -8175/T + 11.526 \tag{6}$$

$$\log B = -14541/T - 1.510 \log T + 24.523 \tag{7}$$

$$\log C = -23573/T - 3.020 \log T + 42.024 \tag{8}$$

The saturation vapor pressure of liquid Se could be expressed by

$$\log p^\circ(\Sigma\, Se_n) = -4955/T + 5.175 \text{ (atm)} \tag{9}$$

and the partial pressure of Se_2 by

$$\log p^\circ(Se_2) = -7712/T - 3.927 \log T + 19.340 \text{ (atm)} \tag{10}$$

The parameters A, B, and C were calculated from Eqs. (6) to (8) for each specimen temperature. Since the pressure in the equilibration tube is constant and therefore the total vapor pressure above the specimen at T_S is equal to that of liquid Se at T_R, the total vapor pressure, p, at T_R could be obtained from Eq. (9). The partial pressure of Se_2 in the vapor at T_S was then calculated by inserting the values for A, B, C, and p in Eq. (5) and solving for $p(Se_2)$. This value was divided according to Eq. (1) by $p^\circ(Se_2)$ [from Eq. (10) solved for T_S],

Table 2. *Extrapolated Saturation Partial Pressures* $p°(Se_x)$ (atm)

Temperature	500 °C	550 °C	600 °C	650 °C	685 °C
$p°(Se_2)$	$1.22 \cdot 10^{-2}$	$4.09 \cdot 10^{-2}$	$1.19 \cdot 10^{-1}$	$3.04 \cdot 10^{-1}$	$5.78 \cdot 10^{-1}$
$p°(Se_3)$	$2.30 \cdot 10^{-4}$	$9.70 \cdot 10^{-4}$	$3.58 \cdot 10^{-3}$	$1.12 \cdot 10^{-2}$	$2.33 \cdot 10^{-2}$
$p°(Se_4)$	$5.50 \cdot 10^{-4}$	$2.24 \cdot 10^{-3}$	$8.10 \cdot 10^{-3}$	$2.52 \cdot 10^{-2}$	$5.18 \cdot 10^{-2}$
$p°(Se_5)$	$7.14 \cdot 10^{-3}$	$1.74 \cdot 10^{-2}$	$3.75 \cdot 10^{-2}$	$7.80 \cdot 10^{-2}$	$1.22 \cdot 10^{-1}$
$p°(Se_6)$	$1.26 \cdot 10^{-2}$	$2.82 \cdot 10^{-2}$	$5.73 \cdot 10^{-2}$	$1.08 \cdot 10^{-1}$	$1.60 \cdot 10^{-1}$
$p°(Se_7)$	$4.56 \cdot 10^{-3}$	$9.90 \cdot 10^{-3}$	$2.03 \cdot 10^{-2}$	$3.74 \cdot 10^{-2}$	$5.60 \cdot 10^{-2}$
$p°(Se_8)$	$6.20 \cdot 10^{-4}$	$1.42 \cdot 10^{-3}$	$3.02 \cdot 10^{-3}$	$5.90 \cdot 10^{-3}$	$8.90 \cdot 10^{-3}$
$\Sigma p^0(Se_x)$	$3.79 \cdot 10^{-2}$	$1.01 \cdot 10^{-1}$	$2.49 \cdot 10^{-1}$	$5.70 \cdot 10^{-1}$	$1.00 \cdot 10^{0}$
Temperature	700 °C	750 °C	800 °C	900 °C	1000 °C
$p^0(Se_2)$	$7.33 \cdot 10^{-1}$	$1.56 \cdot 10^{0}$	$3.12 \cdot 10^{0}$	$8.55 \cdot 10^{0}$	$1.64 \cdot 10^{1}$

the partial pressure of Se_2 in the saturated vapor at T_S, to obtain the activity of Se.

Method C is the most direct approach and it is based on the measurements of the temperature dependence of the saturation partial pressures $p°(Se_x)$ ($x = 2$–8) between 200 and 450 °C by a mass spectrometric electrochemical *Knudsen* method* [30]. Since the plots of log $p°(Se_n)$ vs. $1/T$ show little curvature, the curves for $p°(Se_3)$ to $p°(Se_8)$ were extrapolated to the boiling point of Se (685 °C) and for $p°(Se_2)$ to 1000 °C. The extrapolated values, listed in Table 2**, add up to one atm at 685 °C. In order to calculate the Se activities according

Table 3. *Enthalpies of Reaction* $[Se_{x(g)} = (x/2)\ Se_{2(g)}]$

Se_x	$\Delta H_x°$ (kcal/mol Se_x)
Se_3	7.86
Se_4	23.74
Se_5	52.23
Se_6	70.51
Se_7	85.10
Se_8	100.28

to Eq. (1), we again selected Se_2 as the reference species. The total vapor pressure is given by

$$p = p(Se_2) + p(Se_3) + p(Se_4) + p(Se_5) + p(Se_6) + p(Se_7) + p(Se_8) = \\ = \Sigma\, p(Se_x). \tag{11}$$

There are six equations of the kind

$$Se_{x(g)} = (x/2)\ Se_{2(g)} \tag{12}$$

connecting the various molecular species with Se_2, with the equilibrium constants

$$K_x = p(Se_2)^{x/2}/p(Se_x). \tag{13}$$

Combining Eqs. (11) and (13) we get

$$p = p(Se_2) + \sum_{x=3}^{8} p(Se_2)^{x/2}/K_x. \tag{14}$$

* The authors are grateful to Prof. *J. Drowart*, Univ. of Brussels, for making available to them the data before publication.

** The values are in excellent agreement with an independent evalution of *Mills* [27].

Applying the Gibbs-Helmholtz equation with T_R and T_S as limits we obtain

$$K_x(\text{at } T_S) = K_x(\text{at } T_R) \exp\left[(-\Delta H_x^\circ/R)(T_R - T_S)/(T_S \cdot T_R)\right] \quad (15)$$

with ΔH_x° the enthalpies of dissociation of Eqs. (12). K_x (at T_R) can be calculated from Eq. (13) using the known saturation partial

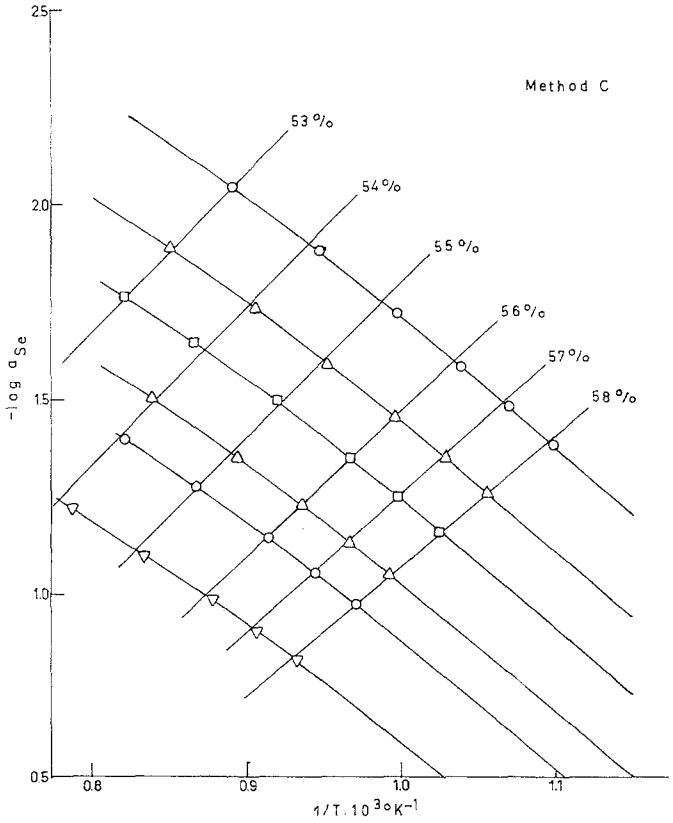

Fig. 3. Activity of Se as a function of temperature

pressures. The ΔH_x° values were obtained from the enthalpies of atomization[30], $\Delta H^\circ_{0,A}(Se_x)$, according to

$$\Delta H_x^\circ = \Delta H^\circ_{0,A}(Se_x) - (x/2)\, \Delta H^\circ_{0,A}(Se_2) \quad (16)$$

and are listed in Table 3. Since the total pressure, p, in the equilibration tube is fixed by T_R, the partial pressures of Se_2, $p(Se_2)$, which are in equilibrium with the specimens can be obtained by combining

Eqs. (14), (15), and (16). The result is an equation of the eighth order which was solved by a computer program (iterative Newton method). The physically meaningful value for $p(Se_2)$ was selected and together with the saturation partial pressure of Se_2, $p^\circ(Se_2)$, taken from the extrapolated vapor pressure curve (Table 2) or from the results of *Keller* et al.[30], introduced in Eq. (1) to calculate the activity of Se.

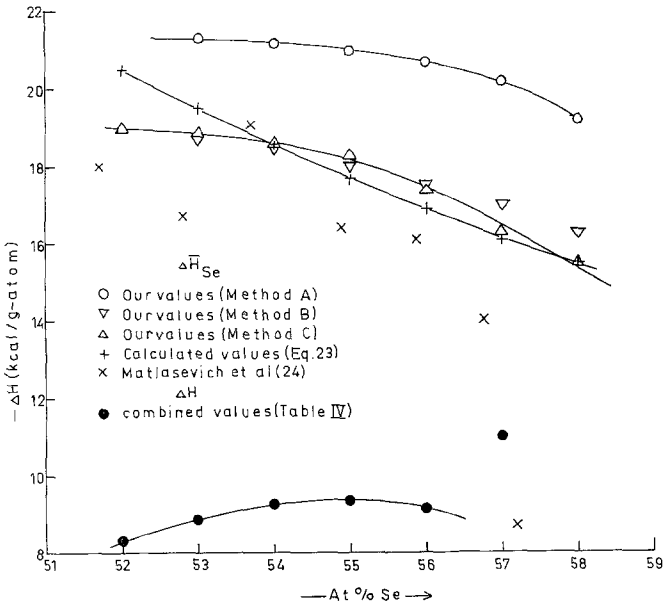

Fig. 4. Partial molar enthalpy of Se and integral molar enthalpy in the $Co_{1-x}Se$ phase

The activities of Se, calculated according to methods A, B, and C are listed in Table 1. Since the complexity of the Se vapor ruled out an evaluation of the partial molar enthalpy of Se according to Eq. (3), the activities were plotted as $\log a_{Se}$ vs. $1/T$, shown in Fig. 3 for method C as an example. For selected compositions temperatures were interpolated on the equilibration curves in Fig. 1 and their reciprocal values plotted on the $\log a_{Se}$ vs. $1/T$ curves in Fig. 3. For a given composition these points lie on a straight line according to

$$\log a_{Se}(\text{at } T_2) - \log a_{Se}(\text{at } T_1) = (\Delta \bar{H}_{Se}/4.575)\,[(1/T_2) - (1/T_1)] \qquad (17)$$

The $\Delta \bar{H}_{Se}$ values, calculated from the slope of these lines, are also listed in Table 1 in kcal/g-atom. Due to the very narrow range of homogeneity of the pyrite phase ($\sim$ 0.3 at% Se) $\Delta \bar{H}_{Se}$ values could

not be calculated for this compound. The partial molar enthalpies of Se obtained by the three methods are shown in Fig. 4.

The $\Delta \overline{H}_{Se}$ values of Table 1 were used to calculate activities of

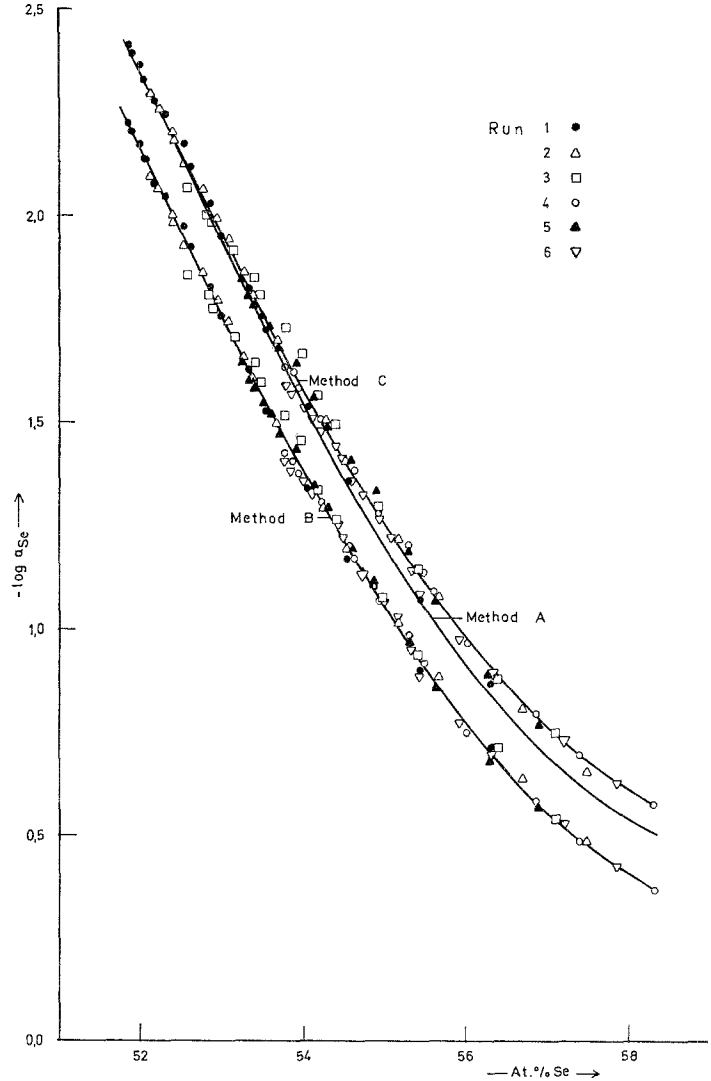

Fig. 5. Activity of Se as a function of composition at 875 °C

Se for given temperatures with Eq. (17). In Fig. 5 the results are compared at 875 °C, with the data points shown only for method B and C. The curves "B" and "C" differ only by about 10% and have the same

slope. Curve "A" is close to curve "C" but has a somewhat steeper slope. Since the $\Delta \bar{H}_{Se}$ values of method B and C (Fig. 4) are the same within the limits of error, a change in temperature will not affect the relative position of curve "B" and "C". The $\Delta \bar{H}_{Se}$ values of method A are, however, more negative and the position of curve "A" in Fig. 5 will shift with changing temperature with respect to curve "B" and "C". The good agreement between curves "A" and "C" in Fig. 5 is therefore fortuitous. In view of the simplifying assumptions the results of method A are actually quite acceptable for a quick evaluation of the experiments. But as the difference in the $\Delta \bar{H}_{Se}$ data (Fig. 4) shows, for an accurate calculation method B or C has to be employed. The agreement between the $\Delta \bar{H}_{Se}$ data of method B and C is excellent and the difference in the activity values, although larger than the spread of the data points, is not excessive. Still, since method C is based on actual measurements of the partial pressures of the various molecular species in the Se vapor, albeit at lower temperatures, preference is given to the results obtained by method C.

The most recent and also the most extensive studies of the thermodynamic properties of solid Co—Se alloys are those of *Laffitte* and *Cerclier*[14, 15] and of *Matlasevich* et al.[24, 25]. Both groups determined the activities of Co in the temperature range between about 400 and 600 °C by *emf* methods, *Laffitte* and *Cerclier* using a solid $BaCl_2$ electrolyte, *Matlasevich* et al. employing a liquid KCl—LiCl—$CoCl_2$ electrolyte. When one compares the two sets of activity data at 600 °C, the agreement is quite good, with the values of *Matlasevich* et al. being somewhat larger. Both sets of data points cluster randomly around previously derived theoretical curves[2]

$$\ln \lambda_{Co} = \ln\left(\frac{1 - 6\,\Delta N_{Se}}{8\,\Delta N_{Se}}\right) - \frac{16\,E_i}{RT}\left(\frac{\Delta N_{Se}}{1 + 2\,\Delta N_{Se}}\right) - \ln K - \frac{E_v}{RT} \qquad (18)$$

with λ_{Co} the absolute activity of Co, E_i the interaction energy between Co vacancies, E_v the energy of formation of a Co vacancy, K the term for the nonconfigurational contribution, and $\Delta N_{Se} = N_{Se} - 0.5$. Between 55 and 58.5 at% Se the sign of the temperature coefficient of the *emf* data of *Laffitte* and *Cerclier*[14, 15] changes with decreasing temperature from positive to negative and the agreement in this range at lower temperatures is therefore less satisfactory. At lower Se concentrations (beginning at 51.5 at% Se) the $\Delta \bar{H}_{Co}$ values of the two groups differ only by 1 kcal and are slightly positive, but they deviate sharply towards strongly negative values at 54.5 at% Se[14, 15], and at 56.5 at% Se[24, 25], resp. The molar enthalpies of formation, obtained

by Gibbs-Duhem integration at 405 °C[15], and at 427 °C[24], are in the average — 8 kcal/g-atom[24] and — 14 kcal/g-atom[15], resp., and in both cases they decrease slightly towards more negative values with increasing Se concentration. The enthalpy of formation of $CoSe_2$ was reported to be — 8.54 kcal/g-atom at 427 °C[24], and — 14.25 kcal/g-atom at 400 °C[15], resp. The *emf* curve of *Laffitte* and *Cerclier*[14, 15] for $CoSe_2$ is composed of two straight branches. There is no indication in the phase diagram[18] that $CoSe_2$ is in equilibrium with a different phase above 450 °C which might explain the shape of the *emf* curve. Possibly the measurements at higher temperatures could have been affected either by a loss of Se from the specimens by evaporation or by the formation of a low melting eutectic at 495 °C in the $BaCl_2$—$CoCl_2$ system[35]. *Mills*[27] calculated enthalpies of formation of Co—Se alloys at 25 °C from the free energy data of *Laffitte* and *Cerclier* at 405 °C and from estimated standard entropies by a Third Law evaluation. He obtained for an alloy with 51.7 at% Se $\Delta H^\circ_{298} = -7.38$ kcal/g-atom, for an alloy with 54.6 at% Se $\Delta H^\circ_{298} = -7.68$ kcal/g-atom, and for $CoSe_2$ $\Delta H^\circ_{298} = -7.46$ kcal/g-atom. Since these values, taking into account the enthalpy of fusion of Se, are in very good agreement with the enthalpies of formation of *Matlasevich* et al.[24, 25], the ΔH data of *Laffitte* and *Cerclier*, obtained by a Second Low evaluation, seem to be in error.

For a direct comparison with our data activities and partial molar enthalpies of Se were calculated by Gibbs-Duhem integration at the intermediate temperature of 600 °C and are plotted in Fig. 6. The activities of Se, calculated directly from the partial molar values of *Cerclier*[15], do not agree with our results. However, by using our activity of Se at 58.5 at% Se obtained by method B or C as limiting value and then performing the Gibbs-Duhem integration, the agreement with the data of *Cerclier*[15] for alloys between 51 and 56 at% Se is very good. The $\log a_{Se}$ data of *Matlasevich* et al.[24] are less negative than ours but the shape of the curve is the same. Taking into account the uncertainties of the Gibbs-Duhem integration and the extrapolation involved, the agreement is satisfactory. The $\Delta \bar{H}_{Se}$ values of *Matlasevich* et al.[24], shown in Fig. 4, are also in good agreement with our data. The $\Delta \bar{H}_{Se}$ values of *Cerclier*[15], not shown in Fig. 4, are much more negative (— 30 to — 28 kcal/g-atom) between 51.5 and 54.5 at% Se and then change abruptly to — 12 kcal/g-atom at 56 at% Se.

Feenberg and *Vaisburd*[26] determined activities of Co in liquid Co—Se alloys at 1300 °C with an *emf* method using the cell $Co_{(s)}$/silicate melt + Co^{2+}/Al_2O_3/silicate melt + Co^{2+}/Co—$Se_{(l)}$. The activity of Co decreases from 1.0 at about 35 at% Se to 0.1 at about 50 at% Se, in agreement with the phase diagram[18] which shows a two phase region

α-Co + L_2 extending to about 35 at% Se at 1300 °C. Since no partial molar enthalpies were reported for the liquid Co—Se alloys, the data cannot be compared with the results on solid alloys.

Eror and *Wagner*[23] measured Se vapor pressures between 636 and 780 °C in the two phase regions $Co_{1-x}Se_{(s)}$—$CoSe_{2(s)}$ and $CoSe_{2(s)}$—$Se_{(l)}$

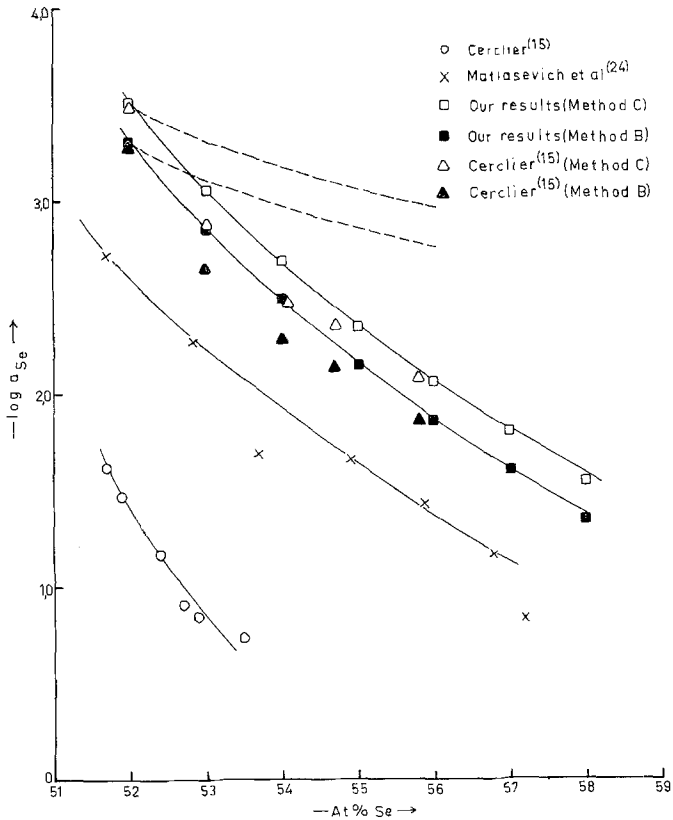

Fig. 6. Activity of Se as a function of composition at 600 °C

and evaluated the activities of Se by treating the vapor as consisting only of Se atoms or of Se_2 molecules. The latter values for the two phase region $Co_{1-x}Se$—$CoSe_2$ can be compared with our data at the $Co_{1-x}Se/Co_{1-x}$—$CoSe_2$ phase boundary evaluated according to method A. The results for three temperatures with the data of *Eror* and *Wagner*[23] in parentheses are as follows: $a_{Se} = 0.037$ (0.016) at 636 °C, $a_{Se} = 0.076$ (0.044) at 703 °C, $a_{Se} = 0.15$ (0.12) at 780 °C. The values of *Eror* and *Wagner* are lower than ours but become less so with in-

creasing temperature. Dissociation pressures of Co—Se alloys between 700 and 1050 °C have been measured with a Bourdon gauge by *Igaki* and *Noda*[16, 17]. They constructed a p—T phase diagram in which nonstoichiometric $Co_{1-x}Se$ is replaced by the three compounds $CoSe_{1.03}$ (50.7 at% Se), $CoSe_{1.13}$ (53.0 at% Se), and $CoSe_{1.30}$ (56.5 at% Se), each with a very narrow range of homogeneity and each ordered up to the melting point. This is at variance with the phase diagram[18] and with the smooth activity—composition curves obtained in this study and by *Laffitte* and *Cerclier*[14, 15] and *Matlasevich* et al.[24]. The partial pressures for the $CoSe_{1.30}$—$CoSe_2$ two phase region[16, 17] can be compared with the data of *Eror* and *Wagner*[23] for the $Co_{1-x}Se$—$CoSe_2$ two phase field. At 636 °C the values are $p \Sigma Se = 3$ mm Hg[16, 17] and 0.1 mm Hg[23], resp., and at about 880 °C the values are the same ($p \Sigma Se \simeq 500$ mm Hg).

The activities and partial molar enthalpies of Se of the present investigation (method C) were combined with the corresponding data for Co of *Matlasevich* et al.[24] to give the integral thermodynamic data for the $Co_{1-x}Se$ phase at 600 °C. The data were taken from smoothed curves at selected compositions and are listed in Table 4. Between 52 and 58 at% Se the integral molar free energy is practically constant. With increasing Se concentration the integral enthalpy of formation ΔH seems to become more negative (Fig. 4), $\Delta \bar{H}_{Se}$ is getting progressively less negative, and $\Delta \bar{H}_{Co}$ (Table 4) is turning towards more negative values. The partial molar enthalpies, however, have not been determined with high enough accuracy so that the concentration dependence of ΔH is somewhat erratic. An independent calorimetric measurement of ΔH would therefore be very desirable.

In two previous papers[1, 2] a model was developed to calculate activities in NiAs-type structures. Assuming a statistical distribution of transition metal atoms and transition metal vacancies in the (001/2) layers of the hexagonal lattice with a certain interaction between the vacancies, equations for the absolute activity of Co, Eq. (18), and by *Gibbs-Duhem* integration for the absolute activity of Se, λ_{Se}, have been derived:

$$\ln \lambda_{Se} = \ln \left\{ \frac{\Delta N_{Se}}{[N_{Se}(0.666 - N_{Se})]^{1/2}} \right\} - \frac{4 E_i}{RT} \left(\frac{1 - 2 N_{Se}}{2 N_{Se}^2} \right) + \text{const.} \qquad (19)$$

Activities of Se were calculated at 600 °C by using the experimental activity at 52 at% Se obtained by method B and C, resp., as the reference point. The dashed curves in Fig. 6 are the values without interaction between the vacancies, i.e. ignoring the term containing E_i

Table 4. *Thermodynamic Properties of the* $Co_{1-x}Se$ *Phase at* 600 °C *(Standard States:* $Co_{(s)}$ *and* $Se_{(l)}$*)*

at% Se	$-\log a_{Se}$ (exp.)	$-\log a_{Co}$ (exp.)	$-\Delta\bar{H}_{Se}$ (kcal/g-atom)	$-\Delta\bar{H}_{Co}$ (kcal/g-atom)	$-\Delta H$ (kcal/g-atom)	$-\Delta G$ (kcal/g-atom)	ΔS (e.u.)	$-\Delta\bar{H}_{Se}$(calc.) (kcal/g-atom)	$-\Delta\bar{S}_{Se}$(exp.) (e.u.)	$-\Delta\bar{S}_{Se}$(calc.) (e.u.)
52.0	3.50	0.78	19.0	— 3.4	8.25	8.87	0.71	20.5	5.75	7.41
53.0	3.06	1.26	18.8	— 2.3	8.88	8.83	— 0.06	19.5	7.54	8.26
54.0	2.69	1.68	18.6	— 1.7	9.26	8.87	— 0.45	18.5	9.00	8.89
55.0	2.34	2.08	18.3	— 1.6	9.35	8.91	— 0.50	17.7	10.26	9.40
56.0	2.03	2.44	17.4	— 1.4	9.12	8.83	— 0.33	16.9	10.64	9.83
57.0	1.77	2.80	16.3	+ 4.0	11.01	8.83	— 2.50	16.1	10.57	10.22
58.0	1.57	3.14	15.5	—	—	8.91	—	15.5	10.57	10.57

in Eq. (19). The solid lines in Fig. 6 are the smoothed experimental values and the square boxes (□ and ■) are the data obtained from Eq. (19) with an interaction energy $E_i = 7780$ cal/g-atom for both method B and C. The agreement between the experimental and theoretical values is excellent, although the symmetry of the phase changes continuously at 53.5 at% Se from hexagonal to monoclinic[13].

A further consequence of the model is the composition dependence of the partial molar enthalpy. Applying the Gibbs-Helmholtz equation to Eq. (18) we obtain

$$\mathrm{d} \ln \lambda_{\mathrm{Co}} = -\left[(E_v/R) + (16\, E_i/R)\left(\frac{\Delta N_{\mathrm{Se}}}{1 + 2\,\Delta N_{\mathrm{Se}}}\right)\right] \mathrm{d}\,(1/T) \tag{20}$$

Comparing Eq. (20) with

$$\mathrm{d} \ln a_{\mathrm{Co}} = (\Delta \bar{H}_{\mathrm{Co}}/R)\, \mathrm{d}\,(1/T) \tag{21}$$

we get

$$\Delta \bar{H}_{\mathrm{Co}} = -\left[E_v + 16\, E_i \left(\frac{\Delta N_{\mathrm{Se}}}{1 + 2\,\Delta N_{\mathrm{Se}}}\right)\right] \tag{22}$$

By performing a Gibbs-Duhem integration with Eq. (22) we finally obtain

$$\Delta \bar{H}_{\mathrm{Se}} = -4\, E_i \left(\frac{1 - 2\, N_{\mathrm{Se}}}{2\, N_{\mathrm{Se}}^2}\right) + \mathrm{const} \tag{23}$$

Eq. (23) was matched with the experimental $\Delta \bar{H}_{\mathrm{Se}}$ values at 58 at% Se and the values at other compositions were then calculated (Table 4). The theoretical data are in good quantitative agreement with the experimental results (Fig. 4), but seem to exhibit a different change in slope.

Combining Eqs. (19) and (23) we finally get the partial molar entropy

$$\Delta \bar{S}_{\mathrm{Se}} = -R \ln \left\{\frac{\Delta N_{\mathrm{Se}}}{[N_{\mathrm{Se}}\,(0.666 - N_{\mathrm{Se}})]^{1/2}}\right\} + \mathrm{const} \tag{24}$$

The experimental data and the theoretical values, calculated by solving Eq. (24) at 58 at% Se, are listed in Table 4. Although the experimental $\Delta \bar{S}_{\mathrm{Se}}$ data are obtained as the difference of two rather large values, the agreement is satisfactory.

Acknowledgment

The financial support of this investigation by the "Fonds zur Förderung der wissenschaftlichen Forschung" under grant number 1322 is gratefully acknowledged.

References

[1] *M. Ettenberg, K. L. Komarek,* and *E. Miller,* J. Solid State Chem. **1**, 583 (1970).
[2] *R. M. Geffken, K. L. Komarek,* and *E. Miller,* J. Solid State Chem. **4**,153 (1972).
[3] *M. Hansen* and *K. Anderko,* Constitution of Binary Alloys, 2. Aufl. New York: McGraw-Hill. 1958.
[4] *R. P. Elliott,* Constitution of Binary Alloys, First Supplement. New York: McGraw-Hill. 1965.
[5] *F. S. Shunk,* Constitution of Binary Alloys, Second Supplement. New York: McGraw-Hill. 1969.
[6] *U. Hashimoto,* Nippon Kinzoku Gakkai-Shi **2**, 67 (1938); Chem. Abstr. **32**, 7381[5] (1938).
[7] *L. D. Dudkin* and *V. I. Vaidanich,* Fiz. Tverd. Tela **2**, 1526 (1960).
[8] *I. Oftedal,* Z. physik. Chem. **128**, 137 (1927).
[9] *W. F. DeJong* and *H. W. V. Willems,* Physica **7**, 74 (1927).
[10] *W. F. DeJong* and *H. W. V. Willems,* Z. anorg. allgem. Chem. **170**, 241 (1928).
[11] *S. Tengnér,* Z. anorg. allgem. Chem. **239**, 126 (1938).
[12] *B. Lewis* and *N. Elliott,* J. Amer. Chem. Soc. **62**, 3180 (1940).
[13] *F. Bøhm, F. Grønvold, H. Haraldsen,* and *H. Prydz,* Acta Chem. Scand. **9**, 1510 (1955).
[14] *M. Laffitte* and *O. Cerclier,* High Temp.—High Press. **1**, 449 (1969).
[15] *O. Cerclier,* Thèse, Univ. de Provence, France (1971).
[16] *K. Igaki* and *Y. Noda,* Nippon Kinzoku Gakkaishi **33**, 371 (1969); Chem. Abstr. **70**, 109812 n (1969).
[17] *Y. Noda* and *K. Igaki,* ibid. **35**, 1031 (1971); Chem. Abstr. **76**, 28248 e (1972).
[18] *K. L. Komarek* and *K. Wessely,* Mh. Chem. **103**, 896 (1972).
[19] *A. L. N. Stevels,* Philips Res. Rep. Suppl. Nr. **9** (1969).
[20] *L. Cambi, M. Elli,* and *E. Giudici,* La Chim. e L'Ind. **51**, 795 (1969).
[21] *C. Fabre,* Ann. chim. phys. **10**, 472 (1887).
[22] *M. Kh. Karapet'yants,* Trudy M. Kh. T. I. im. D. I. Mendeleeva **20**, 10 (1955).
[23] *N. G. Eror* and *J. B. Wagner, Jr.,* Acta Met. **11**, 1339 (1963).
[24] *O. B. Matlasevich, V. A. Geiderikh,* and *Ya. I. Gerassimov,* Rev. Chim. minér. **9**, 191 (1972).
[25] *O. B. Matlasevich* and *V. A. Geiderikh,* J. Fiz. Khim. **46**, 1829 (1972).
[26] *I. Y. Feenberg* and *S. E. Vaisburd,* J. Fiz. Khim. **46**, 1575 (1972).
[27] *K. Mills,* National Physical Laboratory, Teddington, England, private comm.
[28] *K. L. Komarek* and *G. Stummerer,* Mh. Chem. **102**, 1360 (1971).
[29] *W. F. Roeser* and *S. Lonberger,* Natl. Bur. Std. (U.S.), Circ. No. 590 (1956).

[30] *H. Keller, H. Rickert, D. Detry, J. Drowart,* and *P. Goldfinger,* Z. physik. Chem. [NF] **75**, 273 (1971).
[31] *H. Rau,* Ber. Bunsenges. Physik. Chem. **71**, 711 (1967).
[32] *E. H. Baker,* J. Chem. Soc. **A 1968**, 1089.
[33] *R. F. Brebrick,* J. Phys. Chem. **43**, 3031 (1965).
[34] *L. S. Brooks,* J. Amer. Chem. Soc. **74**, 227 (1952).
[35] *R. Gee* and *R. A. J. Shelton,* Trans. Inst. Min. Metall. (Sect. C: Mineral Process. Extr. Metall.) **80**, C 192 (1971).

Prof. Dr. K. L. Komarek
Institut für Anorganische Chemie
Universität Wien
Währinger Straße 42
A-1090 Wien
Österreich